Low-Dose CT for Renal Calculi Detection Using Spectral Shaping of High Tube Voltage

Niedrigdosis-CT zur Detektion von Nierensteinen mittels spektraler Filterung hoher Röhrenspannung

Authors

Sebastian Gassenmaier[1], Moritz T Winkelmann[1], Jan-Philipp Magnus[1], Andreas Stefan Brendlin[1], Sven S. Walter[1, 2], Saif Afat[1], Christoph Artzner[1], Konstantin Nikolaou[1], Malte Niklas Bongers[1]

Affiliations

1 Department of Diagnostic and Interventional Radiology, Eberhard Karls Universität Tübingen, Germany
2 Department of Radiology, Division of Musculoskeletal Radiology, NYU Grossman School of Medicine, New York

Key words

CT, calcifications/calculi, nephrolithiasis, tin filtration, kidney, radiation

received 16.12.2020
accepted 18.01.2022
published online 10.03.2022

Bibliography

Fortschr Röntgenstr 2022; 194: 1012–1019
DOI 10.1055/a-1752-0472
ISSN 1438-9029

Georg Thieme Verlag KG, Rüdigerstraße 14,
70469 Stuttgart, Germany

Correspondence

PD Dr. Malte Bongers
Abteilung für diagnostische und interventionelle Radiologie
Tübingen, Universitätsklinikum Tübingen,
Hoppe-Seyler-Straße 3, 72076 Tübingen, Germany
Tel.: +49/70 71/2 98 66 77
Fax: +49/70 71/29 46 38
malte.bongers@med.uni-tuebingen.de

ABSTRACT

Purpose To investigate reduction of radiation exposure in unenhanced CT in suspicion of renal calculi using a tin-filtered high tube voltage protocol compared to a standard low-dose protocol without spectral shaping.

Materials and Methods A phantom study using 7 human renal calculi was performed to test both protocols. 120 consecutive unenhanced CT examinations performed due to suspicion of renal calculi were included in this retrospective, monocentric study. 60 examinations were included with the standard-dose protocol (SP) (100 kV/130 mAs), whereas another 60 studies were included using a low-dose protocol (LD) applying spectral shaping with tin filtration of high tube voltages (Sn150 kV/80 mAs). Image quality was assessed by two radiologists in consensus blinded to technical parameters using an equidistant Likert scale ranging from 1–5 with 5 being the highest score. Quantitative image quality was assessed using regions of interest in abdominal organs, muscles, and adipose tissue to analyze image noise and signal-to-noise ratios (SNR). Commercially available dosimetry software was used to determine and compare effective dose (ED) and size-specific dose estimates (SSDEmean).

Results All seven renal calculi of the phantom could be detected with both protocols. There was no difference regarding calculi size between the two protocols except for the smallest one. The smallest concretion measured 1.5 mm in LD and 1.0 mm in SP (ground truth 1.5 mm). CTDIvol was 3.36 mGy in LD (DLP: 119.3 mGycm) and 8.27 mGy in SP (DLP: 293.6 mGycm). The mean patient age in SP was 47 ± 17 years and in LD 49 ± 13 years. Ureterolithiasis was found in 33 cases in SP and 32 cases in LD. The median concretion size was 3 mm in SP and 4 mm in LD. The median ED in LD was 1.3 mSv (interquartile range (IQR) 0.3 mSv) compared to 2.3 mSv (IQR 0.9 mSv) in SP ($p < 0.001$). The SSDEmean of LD was also significantly lower compared to SP with 2.4 mGy (IQR 0.4 mGy) vs. 4.8 mGy (IQR 2.3 mGy) ($p < 0.001$). The SNR was significantly lower in LD compared to SP ($p < 0.001$). However, there was no significant difference between SP and LD regarding the qualitative assessment of image quality with a median of 4 (IQR 1) for both groups ($p = 0.648$).

Conclusion Tin-filtered unenhanced abdominal CT for the detection of renal calculi using high tube voltages leads to a significant reduction of radiation exposure and yields high diagnostic image quality without a significant difference compared to the institution's standard of care low-dose protocol without tin filtration.

Key Points:

- Tin-filtered CT for the detection of renal calculi significantly reduces radiation dose.
- The application of tin filtration provides comparable diagnostic image quality to that of SP protocols.
- An increase in image noise does not hamper diagnostic image quality.

Citation Format

- Gassenmaier S, Winkelmann MT, Magnus J et al. Low-Dose CT for Renal Calculi Detection Using Spectral Shaping of High Tube Voltage. Fortschr Röntgenstr 2022; 194: 1012–1019

ZUSAMMENFASSUNG

Ziel Ziel dieser Studie war die Untersuchung der Strahlendosisreduktion in der nativen Computertomografie (CT) bei Verdacht auf Nephro- und Urolithiasis mittels additiver Zinn-Filterung im Vergleich zum Standardprotokoll ohne spektrale Filterung.

Material und Methoden Es wurde eine Phantomstudie mit 7 humanen Nierensteinen durchgeführt. Zusätzlich wurden 120 konsekutive, native CT-Untersuchungen, die aufgrund des Verdachts auf Nierensteine durchgeführt wurden, in diese retrospektive, monozentrische Studie aufgenommen. 60 Untersuchungen wurden mit dem Standarddosisprotokoll (SP) (100 kV/130 mAs) durchgeführt, während weitere 60 Untersuchungen mit einem Niedrigdosisprotokoll (LD) mit additiver Zinn-Filterung (Sn150 kV/80 mAs) durchgeführt wurden. Die Bildqualität wurde in consensus durch 2 Radiologen (verblindet für die Akquisitionstechnik) anhand einer äquidistanten Likert-Skala von 1 bis 5 bewertet (5 = sehr gut). Die quantitative Bildqualität wurde mittels Region-of-interest-Analysen in den Bauchorganen sowie im Muskel- und Fettgewebe beurteilt und in Form des Bildrauschens und des Signal-Rausch-Verhältnisses (SNR) verglichen. Zur Analyse der Strahlendosis-Exposition kam eine kommerziell erhältliche Dosimetrie-Software zum Einsatz.

Ergebnisse Alle 7 Nierensteine des Phantoms konnten mit beiden Protokollen nachgewiesen werden. Hinsichtlich der Größe der Konkremente gab es keinen Unterschied zwischen den beiden Protokollen, mit Ausnahme des kleinsten Konkrements. Das kleinste Konkrement maß 1,5 mm in LD und 1,0 mm in SP (Ground Truth 1,5 mm). CTDIvol betrug 3,36 mGy in LD (DLP: 119,3 mGycm) und 8,27 mGy in SP (DLP: 293,6 mGycm). Das mittlere Patientenalter bei SP betrug 47 ± 17 Jahre und bei LD 49 ± 13 Jahre. Eine Ureterolithiasis wurde in 33 Fällen bei SP und in 32 Fällen bei LD gefunden. Die mediane Größe des Konkrements betrug 3 mm bei SP und 4 mm bei LD. Die mediane effektive Dosis (ED) bei LD betrug 1,3 mSv (Interquartilenabstand (IQR) 0,3 mSv) im Vergleich zu 2,3 mSv (IQR 0,9 mSv) bei SP ($p < 0{,}001$). Die Schätzung der diameterkorrigierten Dosis (SSDEmean) bei LD war mit 2,4 mGy (IQR 0,4 mGy) im Vergleich zu 4,8 mGy (IQR 2,3 mGy) bei SP ebenfalls signifikant niedriger ($p < 0{,}001$). SNR war bei LD im Vergleich zur SP signifikant niedriger ($p < 0{,}001$). Hinsichtlich der qualitativen Beurteilung der Bildqualität gab es jedoch keinen signifikanten Unterschied zwischen SP und LD mit einem Median von 4 (IQR 1) für beide Gruppen ($p = 0{,}648$).

Schlussfolgerung Die native CT mit additiver Zinn-Filterung zur Detektion von Nierensteinen führt zu einer signifikanten Reduktion der Strahlendosis im Vergleich zum Standard Low-Dose-Protokoll bei gleichbleibender diagnostischer Aussagekraft.

Kernaussagen:

- Signifikante Reduktion der Strahlendosis mittels Zinn-gefilterter CT zur Detektion von Nierensteinen
- Vergleichbare diagnostische Aussagekraft der Niedrigdosis-CT trotz Anwendung von Zinn-Filterung
- Keine Kompromittierung der diagnostischen Bildqualität durch Anstieg des Bildrauschens

Introduction

Nephrolithiasis is a common disease with a reported prevalence in the Western world ranging from 1–20 % [1–3]. Despite clinical symptoms, medical history, and laboratory results, imaging plays a pivotal role in the diagnosis of nephrolithiasis and urolithiasis. The imaging modalities that are primarily involved are ultrasound (US) and unenhanced computed tomography (CT) [1]. Other imaging methods such as kidney-ureter-bladder radiography or intravenous radiography are currently not the first choice despite their relatively high sensitivity and specificity [1, 3]. US is a relatively cost-effective and vastly available method with good specificity, but low sensitivity [1, 4]. Furthermore, an overestimation of stone size was reported using ultrasound [4]. The superiority of unenhanced CT compared to intravenous urography has already been demonstrated [5]. Due to the fast and less invasive imaging process, CT is well suited for the diagnosis of nephro- and urolithiasis by providing the exact location of the concretion and is therefore considered to be the reference standard [1, 6, 7]. Additionally, the application of dual-energy CT allows the characterization of the material composition of the calculi [8]. Furthermore, CT imaging provides additional information that can be used for the exclusion of the differential diagnosis of acute flank pain (e. g. choledocholithiasis, appendicitis). The major disadvantage of CT in comparison to US is the radiation exposure of the patient. This is especially relevant as nephrolithiasis often affects people of a young age and recurrence rates of 20 % within 5 years are reported [9, 10]. The feasibility of low-dose CT for renal calculi detection was already shown with several techniques ranging from decreased tube voltage and decreased tube current to different reconstruction algorithms (e. g., iterative reconstruction) [11–15]. Another technical possibility is spectral shaping of the X-ray beam for dose reduction. Spectral shaping leads to a significant reduction of radiation exposure via the absorption of low-energy photons which are primarily absorbed in the subcutaneous adipose tissue and, thus, do not reach the CT detector [16–18]. The successful application of this method was previously shown in several studies in chest imaging and also for renal calculi [16, 18–23]. However, available studies for the detection of renal calculi using a high tube voltage protocol with tin filtration (Sn150 kV) are still rare, especially using only single energy protocols.

Therefore, the purpose of this study was to investigate the reduction of radiation exposure in unenhanced CT with suspicion of renal calculi using a tin-filtered high tube voltage protocol compared to a standard low-dose CT protocol without spectral shaping and its impact on image quality.

Materials and Methods

Study design

This retrospective, monocentric study was approved by the institutional review board with waiver of informed consent.

In total, 120 consecutive unenhanced CT examinations of the abdomen and pelvis, which were performed from November 2019 to June 2020 due to suspected renal calculi before (60 examinations) and after implementation of spectral shaping (60 examinations), were included.

Computed tomography imaging protocol

All examinations were performed using a 3rd-generation dual-source scanner equipped with tin filtration (Siemens Somatom Force, Siemens Healthcare, Erlangen; Germany). After scout acquisition in supine position, patients were scanned in the caudo-cranial direction from the pelvis to the diaphragm. Two different protocols were used for imaging. The mono-institutional standard-dose protocol (SP; within the limits of national recommended radiation dose exposure limits) consisted of a collimation of 192 × 0.6 mm, a tube voltage of 100 kV, and a reference tube current of 130 mAs using automatic tube current modulation. The low-dose (LD) protocol consisted also of a collimation of 192 × 0.6 mm, a tube voltage of 150 kV including tin filtration, and a reference tube current of 80 mAs using automatic tube current modulation. All images were reconstructed in the axial and coronal plane using an advanced modelled iterative reconstruction algorithm (ADMIRE, strength level 3, Siemens Healthineers, Erlangen; Germany) with a medium soft tissue kernel (Br40 d) and a slice thickness of 3 mm.

Image analysis

All imaging studies were reviewed in consensus by two radiologists with three and nine years of experience blinded to clinical and technical information. Image quality was assessed qualitatively using an equidistant Likert scale ranging from 1–5: 1: non-diagnostic; 2: poor image quality; 3: acceptable image quality; 4: good image quality; 5: excellent image quality. Additionally, quantitative image quality was evaluated via image noise using standard deviation of attenuation within a region of interest (ROI) with a size of 2.0 cm^2 in the liver (segment VI), spleen, psoas major muscles (height lumbar vertebrae 2), erector spinae muscles (height lumbar vertebrae 2), and subcutaneous fat. Furthermore, the signal-to-noise ratio (SNR) was calculated using the mean attenuation within a ROI divided by its standard deviation in the spleen, psoas major muscles, and subcutaneous fat.

Renal calculi assessment

All examinations were evaluated regarding the presence of nephrolithiasis and ureterolithiasis. The maximum axial diameter of the largest renal as well as ureteral calculi was noted.

Phantom study

Additionally, a phantom study with seven human urinary calculi ranging in diameter from 4.5–1.5 mm was performed using a cylindric phantom with a diameter of 39 cm which was filled with water. The calculi were placed in the middle of the phantom. The calculi were scanned with both protocols. Calculi size was determined in consensus by the two radiologists mentioned above. Detectability was rated on a Likert scale ranging from 1–5: 1: non-diagnostic; 2: poor detectability; 3: sufficient detectability; 4: good detectability; 5: excellent detectability.

Dosimetry evaluation

Dosimetry analysis was performed using commercially available dosimetry and tracking software (Radimetrics, Bayer, Leverkusen; Germany). The volumetric computed tomography dose index ($CTDI_{vol}$), dose length product (DLP), effective dose (ED), and organ dose were analyzed. Furthermore, to strengthen the quality of the comparison of both cohorts, the water-equivalent diameter (WED) and size-specific dose estimates (SSDE) were noted.

Statistical analysis

Proprietary statistical software was used for analysis (SPSS Statistics Version 26, IBM, Armonk, New York). Normally distributed variables are displayed using mean ± standard deviation. Not normally distributed variables are displayed using median and interquartile range in parentheses.

The SP and LD groups were compared via the student's t-test (age) and the Wilcoxon signed rank test (all parameters except for age). WED_{mean} was tested for equivalence accepting a 5 % difference of the mean as equivalent. P-values below 0.05 were regarded as significant.

Results

Phantom study

All seven renal calculi could be detected with both protocols. There was no difference regarding calculi size between the two protocols except for the smallest one. The smallest concretion measured 1.5 mm in LD and 1.0 mm in SP. Detectability was rated excellent for all concretions except for the smallest one for both protocols. Detectability of the smallest concretion was rated as good in LD and sufficient in SP (▶ **Fig. 1**).

The $CTDI_{vol}$ was 3.36 mGy in LD (DLP: 119.3 mGycm) and 8.27 mGy in SP (DLP: 293.6 mGycm).

Patient characteristics

All patients were successfully evaluated. The mean patient age in SP was 47 ± 17 years (range: 20–87 years) and in LD 49 ± 13 years

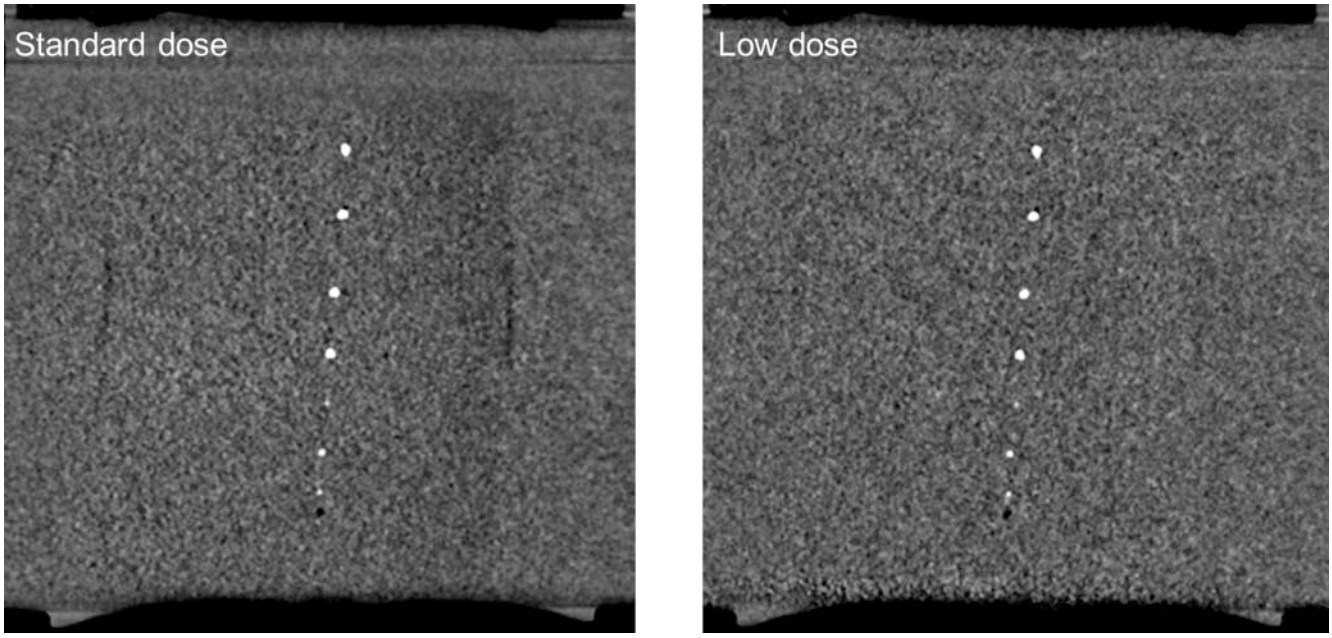

▶ **Fig. 1** Phantom study of seven human renal calculi ranging from 4.5–1.5 mm. Standard-dose imaging (CTDIvol: 8.27 mGy) is shown on the left hand side and low-dose imaging (CTDIvol: 3.36 mGy) on the right hand side. There was no difference between detectability and size measurements between the two protocols except for the smallest concretion. Detectability was rated good in low-dose imaging for the smallest concretion. CTDIvol: Volumetric Computed Tomography Dose Index.

▶ **Abb. 1** Phantomstudie von 7 humanen Nierensteinen mit einer Größe von 4,5–1,5 mm. Auf der linken Seite ist die Standarddosis-Bildgebung (CTDIvol: 8,27 mGy) und auf der rechten Seite die Niedrigdosis-Bildgebung (CTDIvol: 3,36 mGy) dargestellt. Es gab keinen Unterschied zwischen der Erkennbarkeit und den Größenmessungen zwischen beiden Protokollen, außer beim kleinsten Konkrement. Die Erkennbarkeit des kleinsten Konkrements wurde bei der Niedrigdosis-Bildgebung als gut und bei der Standarddosis-Bildgebung als ausreichend bewertet. CTDIvol: Volumetrischer Computertomografie-Dosis-Index.

(range: 26–81 years). Nephrolithiasis was found in 22 patients in SP and in 16 patients in LD (p = 0.327). In both groups, the median calculi size was 4 mm (3 and 2 mm, respectively). There was no significant difference regarding the occurrence of ureterolithiasis (p = 1.000). Further details are displayed in ▶ **Table 1**.

Dosimetry evaluation

The $CTDI_{vol}$, DLP, and ED were significantly lower in LD compared to SP (all p < 0.001; ▶ **Table 2**). The median ED in LD was 1.3 mSv (0.3 mSv) compared to 2.3 mSv (0.9 mSv) in SP. The $SSDE_{mean}$ of LD was also significantly smaller compared to SP with 2.4 mGy (0.4 mGy) vs. 4.8 mGy (2.3 mGy) (p < 0.001). There was no significant difference regarding patient size with WED_{mean} of 29.9 cm (4.5 cm) in SP vs. 31.3 cm (3.8 cm) in LD (p = 0.160). However, the WED_{mean} was not equivalent between the two groups (p = 0.109).

Organ dose evaluation showed significantly lower radiation exposure in LD compared to SP in abdominal organs, e. g., liver organ dose, with 4.1 mSv (1.5 mSv) in SP vs. 2.2 mSv (0.5 mSv) in LD (p < 0.001). Further information is displayed in ▶ **Table 3**.

Qualitative and quantitative image quality

There was no significant difference between SP and LD regarding the qualitative assessment of image quality on a Likert scale with a median of 4 (1) for both groups (p = 0.648). ▶ **Fig. 1** displays an example of a patient who was examined at two different points in time with the SP and LD protocols for a recurrent clinical indication.

Quantitative image analysis revealed slightly higher noise in LD imaging. The standard deviation of attenuation in the liver was 15.3 HU (2.5 HU) in SP vs. 17.0 HU (3.2 HU) in LD (p < 0.001) and in the spleen 15.0 HU (2.2 HU) in SP vs. 17.0 HU (3.1 HU) in LD (p < 0.001; ▶ **Table 4**). Subcutaneous fat showed no significant difference regarding image noise (p = 0.777).

The SNR in the spleen was 3.7 (0.6) in SP compared to 3.0 (0.5) in LD (p < 0.001). The SNR of SP was also significantly higher in psoas major muscles and subcutaneous fat (▶ **Table 4**). ▶ **Fig. 2** shows images of both protocols in the same patient examined at two different points in time.

Discussion

This study could show that reduction of radiation exposure in CT for the detection of renal calculi is feasible using tin filtration at high tube voltages. Although our evaluation showed slightly higher noise levels as well as slightly lower SNR in LD imaging, no significant difference was found regarding diagnostic image quality. This difference might be related to the slightly higher WED in our LD group, as both groups were not equivalent regarding this parameter. Radiation dose evaluation showed a reduction of

▶ **Table 1** Patient characteristics.

▶ **Tab. 1** Patienten-Charakteristika.

Characteristics	Values
Standard-dose group	
Patients	N = 60
Mean age ± std.	47 ± 17 years
Range	20–87 years
Male	N = 40 (67 %)
Low-dose group	
Patients	N = 60
Mean age ± std.	49 ± 13 years
Range	26–81 years
Male	N = 33 (55 %)
Findings	
Standard-dose group	
Nephrolithiasis	N = 22
Size of concretion (median; IQR[1])	4 mm (4 mm)
Ureterolithiasis	N = 33
Size of concretion (median; IQR)	3 mm (2 mm)
Low-dose group	
Nephrolithiasis	N = 16
Size of concretion (median; IQR)	4 mm (3 mm)
Ureterolithiasis	N = 32
Size of concretion (median; IQR)	4 mm (2 mm)

[1] IQR: interquartile range.
IQR: Interquartilenabstand.

approximately 49 % of the $CTDI_{vol,}$ 43 % of the ED, and 50 % of the $SSDE_{mean}$ using the LD protocol compared to the SP protocol.

Our study is in line with the results of Mozaffary et al. who used a similar protocol with tin filtration and a slightly higher tube current [20]. Mozaffary et al. did not find any significant difference regarding image noise between the standard-dose protocol and tin filtration. However, in our study slightly higher noise levels were found in LD imaging. This might be due to further tube current reduction to 80 mAs (compared to 100 mAs in the study of Mozaffary et al.) [20]. An advantage of this 20 mAs tube current reduction is of course a further decrease of radiation exposure. Therefore, the radiation dose in the study by Mozaffary et al. was slightly higher with a $CTDI_{vol}$ of 2.9 ± 0.3 mGy. The radiation exposure in our study was slightly lower compared to Apfaltrer et al. who used the same tube voltage and tube current settings with a $CTDI_{vol}$ of 2.5 ± 1.9 mGy versus 2.2 ± 0.71 mGy in our study [24]. Additionally, in this mentioned study, the SNR was not significantly different in most tissues between low dose and standard dose. However, in our study, a significantly lower SNR was found for LD compared to SP. This might be due to different patient character-

▶ **Table 2** Dosimetry evaluation.

▶ **Tab. 2** Dosisauswertung.

	Standard dose[1]	Low dose[1]	p-value
$CTDI_{vol}$ (mGy)	4.1 (2.7)	2.1 (0.6)	< 0.001
DLP (mGy*cm)	160 (108)	85 (29)	< 0.001
ED (mSv)	2.3 (0.9)	1.3 (0.3)	< 0.001
$SSDE_{min}$ (mGy)	3.7 (1.7)	2.1 (0.3)	< 0.001
$SSDE_{mean}$ (mGy)	4.8 (2.3)	2.4 (0.4)	< 0.001
$SSDE_{max}$ (mGy)	6.7 (4.0)	3.0 (0.5)	< 0.001
WED_{min} (cm)	28.6 (4.7)	29.3 (3.8)	0.420
WED_{mean} (cm)	29.9 (4.5)	31.3 (3.8)	0.179
WED_{max} (cm)	31.6 (5.1)	33.1 (4.0)	0.170

Abbreviations: $CTDI_{vol}$: volumetric computed tomography dose index; DLP: dose length product; SSDE: size-specific dose estimates; WED: water-equivalent diameter.
Abkürzungen: $CTDI_{vol}$:Volumetrischer Computertomografie-Dosis-Index; DLP: Dosislängenprodukt; SSDE: Größenspezifische Dosis Schätzwerte; WED: Wasseräquivalenter Diameter.
[1] Values are given as median (interquartile range).
Werte als Median (Interquartilenabstand).

▶ **Table 3** Organ dose evaluation in millisievert.

▶ **Tab. 3** Evaluation der Organdosen in Millisievert.

	Standard dose[1]	Low dose	p-value[2]
Adrenals	3.4 (1.3)	1.9 (0.5)	< 0.001
Kidneys	5.6 (1.7)	2.7 (0.4)	< 0.001
Liver	4.1 (1.5)	2.2 (0.5)	< 0.001
Spleen	4.2 (1.4)	2.3 (0.5)	< 0.001
Pancreas	3.5 (1.0)	1.9 (0.4)	< 0.001
Stomach	4.7 (1.5)	2.4 (0.4)	< 0.001
Colon	4.4 (1.3)	2.3 (0.4)	< 0.001
Small intestine	4.5 (1.4)	2.4 (0.3)	< 0.001
Urinary bladder	5.0 (1.4)	2.5 (0.4)	< 0.001
Red bone marrow	1.9 (0.6)	1.1 (0.2)	< 0.001
Skin	2.0 (1.2)	1.1 (0.3)	< 0.001
Testicles	0.7 (0.7)	0.5 (0.6)	0.018
Ovaries	4.2 (1.8)	2.3 (0.4)	< 0.001
Uterus	4.4 (1.6)	2.3 (0.3)	< 0.001

[1] Values are given as median (interquartile range).
Werte als Median (Interquartilenabstand).
[2] Statistischer Test: Wilcoxon signed rank test.
Statistical test: Wilcoxon signed rank test.

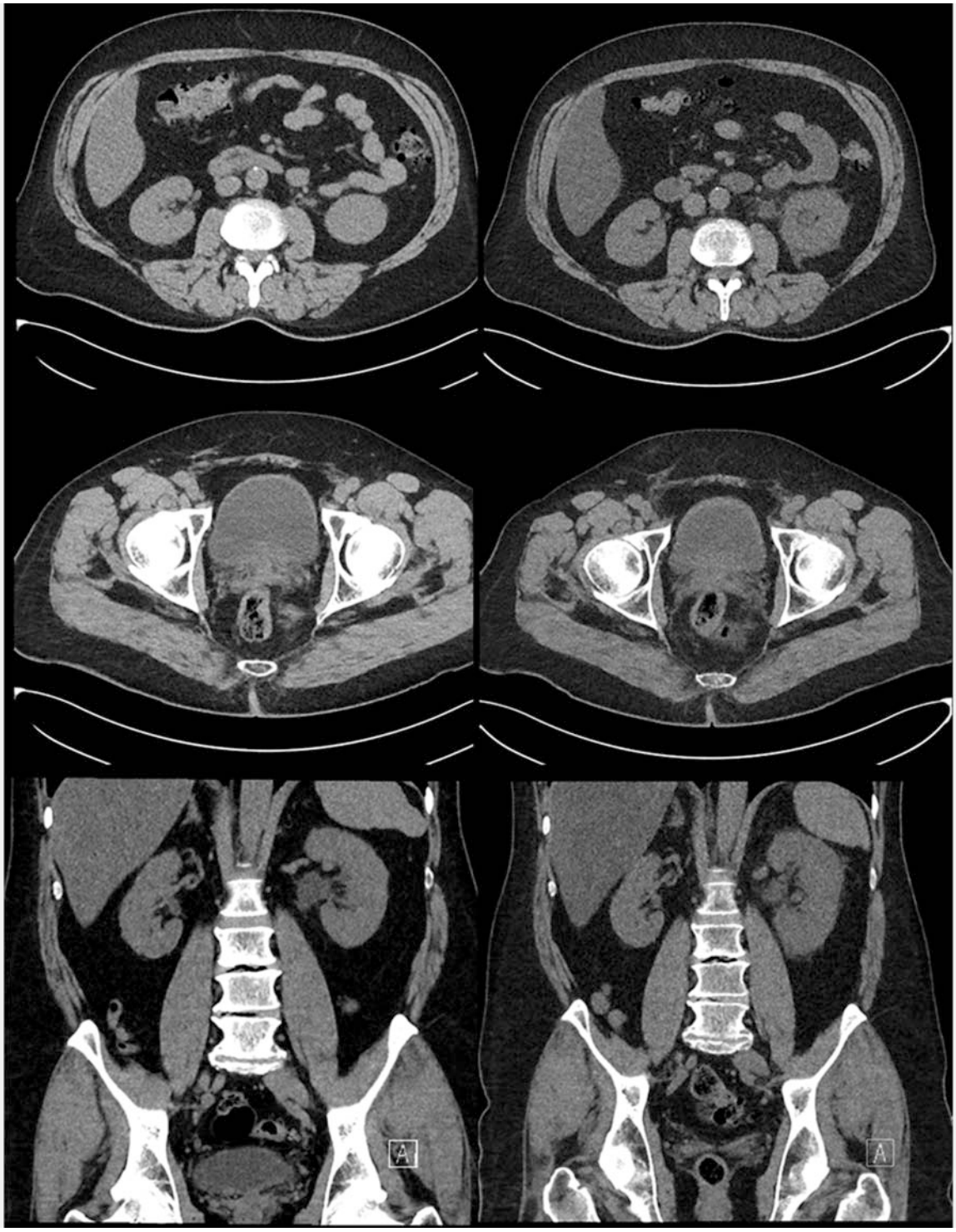

▶ **Fig. 2** shows a 60-year-old male patient who was scanned with the standard-dose protocol (left column) and low-dose protocol (right column) as clinically indicated due to flank pain at two different time points. Despite slightly higher noise levels in low-dose acquisition, both protocols provided high diagnostic image quality. **Dosimetry:** SP: CTDIvol: 6.9 mGy; ED: 3.1 mSv; WEDmean: 34.2 cm; SSDEmean: 7.1 mGy; LD: CTDIvol: 2.8 mGy; ED: 1.6 mSv; WEDmean: 35.0 cm; SSDEmean: 2.8 mGy. Abbreviations: SP = Standard dose; ED: Effective dose; WED: water-equivalent diameter; SSDE: size-specific dose estimate; LD: Low dose.

▶ **Abb. 2** zeigt einen 60-jährigen männlichen Patienten, der sowohl mittels Standardprotokoll (linke Spalte) als auch mit dem Niedrigdosisprotokoll (rechte Spalte) aus klinischer Indikation aufgrund von Flankenschmerzen an 2 unterschiedlichen Zeitpunkten untersucht wurde. Trotz gering höheren Rauschens in der Niedrigdosisuntersuchung besteht weiterhin eine sehr gute Bildqualität. **Dosimetrie:** SP: CTDIvol: 6.9 mGy; ED: 3.1 mSv; WEDmean: 34.2 cm; SSDEmean: 7.1 mGy; LD: CTDIvol: 2.8 mGy; ED: 1.6 mSv; WEDmean: 35.0 cm; SSDEmean: 2.8 mGy. Abkürzungen: SP: Standarddosis; ED: Effektive Dosis; SSDE: size specific dose estimate; WED: water equivalent diameter; LD: Niedrigdosis.

▶ **Table 4** Quantitative image quality assessment using standard deviation of attenuation within a region of interest (noise) (median (interquartile range)) as well as signal-to-noise ratio (SNR).

▶ **Tab. 4** Quantitative Bildqualitätsanalyse mittels Standardabweichung der Dichtewerte innerhalb einer Region of interest (Rauschen) sowie mittels Signal-zu-Rausch-Verhältnis (SNR).

	Standard dose[1]	Low dose[1]	p-value[2]
Noise assessment			
Liver	15.3 (2.5)	17.0 (3.2)	< 0.001
Spleen	15.0 (2.2)	17.0 (3.1)	< 0.001
Psoas major muscles	16.1 (2.5)	17.8 (3.5)	0.001
Erector spinae muscles	15.9 (2.8)	17.8 (3.4)	0.003
Subcutaneous fat	13.2 (2.1)	13.5 (2.4)	0.777
SNR assessment			
Spleen	3.7 (0.6)	3.0 (0.5)	< 0.001
Psoas major muscles	3.4 (0.5)	2.8 (0.7)	< 0.001
Subcutaneous fat	–8.8 (1.9)	–7.0 (1.4)	< 0.001

[1] Values are given as median (interquartile range).
Werte als Median (Interquartilenabstand).
[2] Statistischer Test: Wilcoxon signed rank test.
Statistical test: Wilcoxon signed rank test.

istics. In contrast to the present study, in the investigation of Dewes et al., there was also no significant difference regarding SNR between an Sn150 kV protocol and another non-tin-filtered low-dose protocol using a third-generation dual source scanner [25]. This different finding might be due to the patients' characteristics and differences in the standard low-dose protocol with different tube voltage and tube current settings. Another factor might be the slightly higher WED in our LD group compared to SP patients. Regarding diagnostic image quality, there was no deterioration of image quality in LD acquisition in our study, which is similar to previous examinations with tin filtration [20, 24–26].

The results of this study indicate that at a high tube voltage of Sn150 kV, the tube current might be further lowered. Although, this leads to higher noise levels and a lower SNR, the diagnostic image quality was still unaffected in our investigation. Further studies will be necessary to identify the cut-off of maximum possible tube current reduction without compromised diagnostic image quality. Another factor influencing further radiation exposure is the development and technical improvement of scanner architecture, of course. Despite already low radiation exposure levels, a further decrease would be desirable as recurrence of nephrolithiasis is a common issue and affected patients are often of a young age [1, 10]. Additionally, the basic concepts of radiation protection such as the ALARA principle (as low as reasonably achievable) are always mandatory.

This study has several limitations. All patients were included retrospectively at one imaging center. The presence of urinary calculi was not proven by obtaining the calculi. However, the location of the calculi within the course of the ureter as well as the typical clinical presentation of patients highly suggest the presence of renal calculi. Furthermore, no patient underwent imaging twice with both protocols at the same point in time under study conditions due to radiation exposure concerns. Therefore, no comparison of sensitivity and specificity as well as of stone size is feasible. However, the phantom study showed excellent performance of the low-dose protocol. Only one CT scanner was used in this study setting using a mono-institutional standard protocol for comparison. Furthermore, dosimetry evaluation was also performed using SSDE to overcome this issue. Additionally, although the WED was not equivalent (WED slightly higher in LD compared to SP), there was no significant difference between the two patient cohorts.

Conclusion

This study was able to show that tin-filtered unenhanced abdominal CT for the detection of renal calculi using high tube voltages leads to a significant reduction of radiation exposure and yields sufficient image quality without significant differences compared to a standard of care low-dose CT protocol without tin filtration.

CLINICAL RELEVANCE:

- Tin-filtered CT with a high tube voltage allows a significant radiation dose reduction to a median effective dose of 1.3 mSv.
- Radiation dose evaluation in patients showed a reduction of approximately 49 % of the $CTDI_{vol}$, 43 % of the effective dose, and 50 % of the size-specific dose estimates using the low-dose protocol compared to the standard-dose protocol.
- Qualitative image quality evaluation revealed no significant difference between low-dose and standard-dose CT protocols.
- Further tube current reduction might be possible although increasing noise levels and loss of signal-to-noise ratio must be thoroughly observed.

Conflict of Interest

The authors declare that they have no conflict of interest.

References

[1] Turk C, Petrik A, Sarica K et al. EAU Guidelines on Diagnosis and Conservative Management of Urolithiasis. Eur Urol 2016; 69: 468–474

[2] Stamatelou KK, Francis ME, Jones CA et al. Time trends in reported prevalence of kidney stones in the United States: 1976–1994. Kidney Int 2003; 63: 1817–1823

[3] Hesse A, Brandle E, Wilbert D et al. Study on the prevalence and incidence of urolithiasis in Germany comparing the years 1979 vs. 2000. Eur Urol 2003; 44: 709–713

[4] Ray AA, Ghiculete D, Pace KT et al. Limitations to ultrasound in the detection and measurement of urinary tract calculi. Urology 2010; 76: 295–300

[5] Worster A, Preyra I, Weaver B et al. The accuracy of noncontrast helical computed tomography versus intravenous pyelography in the diagnosis of suspected acute urolithiasis: a meta-analysis. Ann Emerg Med 2002; 40: 280–286

[6] Yilmaz S, Sindel T, Arslan G et al. Renal colic: comparison of spiral CT, US and IVU in the detection of ureteral calculi. Eur Radiol 1998; 8: 212–217

[7] Smith RC, Verga M, McCarthy S et al. Diagnosis of acute flank pain: value of unenhanced helical CT. Am J Roentgenol 1996; 166: 97–101

[8] Spek A, Strittmatter F, Graser A et al. Dual energy can accurately differentiate uric acid-containing urinary calculi from calcium stones. World J Urol 2016; 34: 1297–1302

[9] Rule AD, Lieske JC, Li X et al. The ROKS nomogram for predicting a second symptomatic stone episode. J Am Soc Nephrol 2014; 25: 2878–2886

[10] Ziemba JB, Matlaga BR. Epidemiology and economics of nephrolithiasis. Investig Clin Urol 2017; 58: 299–306

[11] Poletti PA, Platon A, Rutschmann OT et al. Low-dose versus standard-dose CT protocol in patients with clinically suspected renal colic. Am J Roentgenol 2007; 188: 927–933

[12] Niemann T, Kollmann T, Bongartz G. Diagnostic performance of low-dose CT for the detection of urolithiasis: a meta-analysis. Am J Roentgenol 2008; 191: 396–401

[13] Kalra MK, Maher MM, D'Souza RV et al. Detection of urinary tract stones at low-radiation-dose CT with z-axis automatic tube current modulation: phantom and clinical studies. Radiology 2005; 235: 523–529

[14] Khawaja RDA, Singh S, Blake M et al. Ultra-low dose abdominal MDCT: using a knowledge-based Iterative Model Reconstruction technique for substantial dose reduction in a prospective clinical study. Eur J Radiol 2015; 84: 2–10

[15] Rimondini A, Pozzi Mucelli R, De Denaro M et al. Evaluation of image quality and dose in renal colic: comparison of different spiral-CT protocols. Eur Radiol 2001; 11: 1140–1146

[16] Gordic S, Morsbach F, Schmidt B et al. Ultralow-dose chest computed tomography for pulmonary nodule detection: first performance evaluation of single energy scanning with spectral shaping. Invest Radiol 2014; 49: 465–473

[17] Braun FM, Johnson TR, Sommer WH et al. Chest CT using spectral filtration: radiation dose, image quality, and spectrum of clinical utility. Eur Radiol 2015; 25: 1598–1606

[18] Schabel C, Marin D, Ketelsen D et al. Tin-filtered low-dose chest CT to quantify macroscopic calcification burden of the thoracic aorta. Eur Radiol 2018; 28: 1818–1825

[19] Bodelle B, Fischbach C, Booz C et al. Single-energy pediatric chest computed tomography with spectral filtration at 100 kVp: effects on radiation parameters and image quality. Pediatr Radiol 2017; 47: 831–837

[20] Mozaffary A, Trabzonlu TA, Kim D et al. Comparison of Tin Filter-Based Spectral Shaping CT and Low-Dose Protocol for Detection of Urinary Calculi. Am J Roentgenol 2019; 212: 808–814

[21] Gassenmaier S, Schaefer JF, Nikolaou K et al. Forensic age estimation in living adolescents with CT imaging of the clavicula-impact of low-dose scanning on readers' confidence. Eur Radiol 2020; 30: 6645–6652

[22] Haubenreisser H, Meyer M, Sudarski S et al. Unenhanced third-generation dual-source chest CT using a tin filter for spectral shaping at 100kVp. Eur J Radiol 2015; 84: 1608–1613

[23] Vivier S, Deken V, Arous Y et al. Pediatric chest computed tomography at 100 kVp with tin filtration: comparison of image quality with 70-kVp imaging at comparable radiation dose. Pediatr Radiol 2020; 50: 188–198

[24] Apfaltrer G, Dutschke A, Baltzer PAT et al. Substantial radiation dose reduction with consistent image quality using a novel low-dose stone composition protocol. World J Urol 2020; 38: 2971–2979

[25] Dewes P, Frellesen C, Scholtz JE et al. Low-dose abdominal computed tomography for detection of urinary stone disease – Impact of additional spectral shaping of the X-ray beam on image quality and dose parameters. Eur J Radiol 2016; 85: 1058–1062

[26] Zhang GM, Shi B, Sun H et al. High-pitch low-dose abdominopelvic CT with tin-filtration technique for detecting urinary stones. Abdom Radiol (NY) 2017; 42: 2127–2134